Low-Energy Models for Correlated Materials: Bandwidth Renormalization from Coulombic Screening

M. Casula, Ph. Werner, L. Vaugier, F. Aryasetiawan, T. Miyake, A. J. Millis, and S. Biermann

Phys. Rev. Lett. **109**, 126408 — Published 19 September 2012

DOI: 10.1103/PhysRevLett.109.126408

Low-energy models for correlated materials: bandwidth renormalization from Coulombic screening

M. Casula,[1] Ph. Werner,[2] L. Vaugier,[3,4] F. Aryasetiawan,[5] T. Miyake,[6,4] A. J. Millis,[7] and S. Biermann[3,4]

[1]*CNRS and Institut de Minéralogie et de Physique des Milieux condensés, Université Pierre et Marie Curie, case 115, 4 place Jussieu, 75252, Paris cedex 05, France*
[2]*Department of Physics, University of Fribourg, 1700 Fribourg, Switzerland*
[3]*Centre de Physique Théorique, Ecole Polytechnique, CNRS-UMR7644, 91128 Palaiseau, France*
[4]*Japan Science and Technology Agency, CREST, Kawaguchi 332-0012, Japan*
[5]*Department of Physics, Mathematical Physics, Lund University, Sölvegatan 14A, 22362 Lund, Sweden*
[6]*Nanosystem Research Institute (NRI), AIST, Tsukuba, Ibaraki 305-8568, Japan*
[7]*Department of Physics, Columbia University, 538 West, 120th Street, New York, NY 10027, USA*

We provide a prescription for constructing Hamiltonians representing the low energy physics of correlated electron materials with dynamically screened Coulomb interactions. The key feature is a renormalization of the hopping and hybridization parameters by the processes that lead to the dynamical screening. The renormalization is shown to be non-negligible for various classes of correlated electron materials. The bandwidth reduction effect is necessary for connecting models to materials behavior and for making quantitative predictions for low-energy properties of solids.

PACS numbers: 71.27.+a,71.30.+h,71.10.Fd

A key step in the theoretical analysis of strongly correlated materials is the derivation, from an all-electron Hamiltonian in the continuum, of an effective model which correctly captures the physics of the low-energy degrees of freedom. Tremendous progress in this direction has been achieved by using density functional theory (DFT) techniques [1] to compute a full set of energy bands, from which a subset of correlated orbitals is abstracted for further detailed study using many-body (typically dynamical mean field (DMFT)) methods [2–4] or LDA+U. The interaction parameters used in the many-body studies are the matrix elements of the screened Coulomb interaction in the correlated subspace. Various methods are used to obtain the screened matrix elements, including the constrained local density approximation [5], linear response [6], or the constrained random phase approximation (cRPA) [7]. This DFT+DMFT approach enables quantitative, testable theoretical predictions for correlated materials.

In this paper we show that this scheme misses an important aspect of the physics: the downfolding produces a dynamically screened Coulomb interaction which leads to an effective model with a bandwidth that is *reduced* relative to the starting (e.g. DFT) bandwidth and a low energy spectral weight which is also reduced. This effect has previously been noticed [7–10]. A similar renormalization was also discussed in the context of Holstein-Hubbard models in Refs [11, 12]. We present an explicit nonperturbative prescription for determining the renormalizations quantitatively, and demonstrate that the resulting effective model provides a good description of the low-energy part of the full (dynamically interacting) model over wide parameter ranges. Computations of the renormalizations for wide classes of correlated electron materials indicate that their inclusion is crucial for a quantitative description, in particular resolving a long-standing discrepancy between the cRPA estimate of the Coulomb interaction and the values needed to describe experiments.

We first provide a demonstration for the simplest case, where the downfolding from the full band structure is to a one-band model with hopping amplitude t_{ij} between the lattice sites i and j. Electrons with spin σ in the correlated orbital localized at site i are created [annihilated] by the operator $d^\dagger_{i\sigma}$ [$d_{i\sigma}$]. Double occupation of a given atomic site costs a Coulomb energy U, which is renormalized from a bare value V (obtained from the site-local matrix elements of e^2/r among the correlated orbitals) because of screening by degrees of freedom eliminated in the downfolding process. The interaction thus takes the general form $\frac{1}{2}\left(V\delta(\tau)+U_{\rm ret}(\tau)\right)n_i(\tau)n_i(\tau')$, with $n_i(\tau)=d^\dagger_i(\tau)d_i(\tau)$, the local density operator at the imaginary time τ. Screening is contained in the retarded part $U_{\rm ret}$, which is parametrized by a continuum of modes of energy ν with coupling strength $\lambda^2(\nu)=-{\rm Im}U_{\rm ret}(\nu)/\pi$, determined by the charge fluctuations,

$$U_{\rm ret}(\tau) = -\int_0^\infty {\rm d}\nu\lambda^2(\nu)\cosh[(\tau-\beta/2)\nu]/\sinh[\nu\beta/2], \tag{1}$$

where β is the inverse temperature. For simplicity of presentation we assume at first that there is only one important bosonic mode of energy ω_0 and coupling strength λ. The Hamiltonian is then

$$\begin{aligned} H = &-\sum_{ij\sigma} t_{ij} d^\dagger_{i\sigma} d_{j\sigma} + V\sum_i d^\dagger_{i\uparrow}d_{i\uparrow}d^\dagger_{i\downarrow}d_{i\downarrow} + \mu\sum_{i\sigma} d^\dagger_{i\sigma}d_{i\sigma} \\ &+ \omega_0\sum_i b^\dagger_i b_i + \lambda\sum_{i\sigma} d^\dagger_{i\sigma}d_{i\sigma}(b_i+b^\dagger_i). \end{aligned} \tag{2}$$

A Lang-Firsov (LF) transformation [13, 14] $H \to H_{LF} = e^S H e^{-S}$ with $S = \frac{\lambda}{\omega_0} \sum_{i\sigma} n_{i\sigma}(b_i + b_i^\dagger)$ allows one to rewrite the model in terms of the polaron operators $c_{i\sigma}^\dagger = \exp(\frac{\lambda}{\omega_0}(b_i^\dagger - b_i))d_{i\sigma}^\dagger$ and $c_{i\sigma} = \exp(\frac{\lambda}{\omega_0}(b_i - b_i^\dagger))d_{i\sigma}$. We note that c and $c^\dagger$ obey the same fermionic anti-commutation relations as the original electronic operators (d and $d^\dagger$). Neglecting one-body terms which can be absorbed in a chemical potential shift, we have

$$H_{\rm LF} = -\sum_{ij\sigma} t_{ij} c_{i\sigma}^\dagger c_{j\sigma} + U_0 \sum_i c_{i\uparrow}^\dagger c_{i\uparrow} c_{i\downarrow}^\dagger c_{i\downarrow} + \omega_0 \sum_i b_i^\dagger b_i, \tag{3}$$

with the screened Hubbard interaction $U_0 = V - \frac{2\lambda^2}{\omega_0}$.

We now propose that the low energy effective model is given by *the projection of Eq. (3) onto the subspace of zero-boson states*, $H_{\rm eff} = \langle 0|H|0\rangle$, an assumption based on the separation of plasmon excitations from the low energy spectral properties. This ansatz becomes exact in the limit of infinite plasma frequency and as will be seen gives a remarkably good description for physically relevant values. The effective model is then

$$H_{\rm eff} = -\sum_{ij\sigma} Z_B t_{ij} d_{i\sigma}^\dagger d_{j\sigma} + U_0 \sum_i d_{i\uparrow}^\dagger d_{i\uparrow} d_{i\downarrow}^\dagger d_{i\downarrow}, \tag{4}$$

that is, an effective Hubbard model with an instantaneous interaction corresponding to the low frequency limit of the screened interaction and a new feature, namely a bandwidth renormalized by $Z_B = \exp(-\lambda^2/\omega_0^2)$. An additional physical consequence of the low-energy projection is that the photoemission spectral weight in the frequency range described by the effective model is reduced by the factor Z_B relative to what would naively follow from H_{LF}. Mathematically, $G^{\text{low-energy}}$, the physical electron Green function in the frequency range described by the effective model, is

$$G_{ij}^{\text{low-energy}}(\tau) = -Z_B \langle T d_i(\tau) d_j^\dagger(0)\rangle_{H_{\rm eff}}, \tag{5}$$

where $-\langle T d_i(\tau) d_j^\dagger(0)\rangle_{H_{\rm eff}}$ is the Green's function $G_{ij}^{\rm eff}(\tau)$ of the effective Hamiltonian $H_{\rm eff}$ in Eq. (4). Thus the observable spectral function $A^{\text{low-energy}} = -\frac{1}{\pi}{\rm Im}G^{\text{low-energy}}(\omega - i\delta)$ becomes

$$A^{\text{low-energy}}(\omega) = -\frac{Z_B}{\pi}{\rm Im}G^{\rm eff}(\omega - i\delta). \tag{6}$$

The physical origin is that part of the physical photoemission spectrum corresponds to the simultaneous creation of a hole and a plasmon excitation; these plasmon shakeoff processes account for the remaining $1 - Z_B$ spectral weight.

The effective model becomes an exact description of the low energy physics only when the ratio of the boson frequency ω_0 to a relevant energy E^* diverges, but we find that the effective model gives a reasonably good description even for ω_0/E^* not too large. As an example, Table I compares exact results (obtained using the methods of Ref. [15]) for the critical interaction strength $U_{\rm crit}$ needed to drive a metal-insulator transition in single-site DMFT to the predictions of the effective model. In these computations we assume that the t_{ij} give a semicircular density of states with half-bandwidth $D = 1$. Combining previously computed single site DMFT results [15] with our bandwidth reduction prescription gives, at inverse temperature $\beta = 100/D$, an effective model prediction $U_{\rm crit}^{\rm eff} \approx 2.55 Z_B$. One sees that the effective model result is within 15% of the exact result except when there is strong screening and the boson frequencies are smaller than the full bandwidth (2 in present units).

Figure 1 compares the electron spectral function, calculated from Eq. (2) with semicircular density of states (half bandwidth $D = 1$), for screened interaction $U_0 = 2$ with values of Z_B representative of typical correlated electron materials to two approximations: the effective model defined above, and a "static U model" which uses the static value of the screened Coulomb interaction but does not include the bandwidth reduction. The static U model corresponds to what is normally done in DFT+DMFT calculations. The analytic continuations are obtained using the technique proposed in Ref. [16]. We see that the effective model with bandwidth reduction Z_B reproduces very well the effective bandwidths of the Hubbard bands for all ω_0 taken into account here, which vary from 10 down to 2.5. Even the smallest ω_0, which is not in the antiadiabatic regime, yields Hubbard bands qualitatively well described by the static model with bandwidth renormalization Z_B. The static U model is seen to be a poor approximation.

Table II shows the results of an alternative analysis, carried out at the level of the quasiparticle renormalization $a = 1/(1 - \partial\Sigma/\partial i\omega_n)$, which is obtained directly from the imaginary time computations. We see that the "static U" result gives renormalization factors in error by factors of two or more in the half filled, strongly correlated case, and also unacceptably large errors in the weakly correlated quarter filled case. The effective model (row $\omega_0 = \infty$) is very close to the exact result for all screening frequencies in the weakly correlated quarter-filled case and is reasonably close to the exact result even as the adiabatic limit is approached.

Analogous arguments for a model comprising also itinerant p states, and thus hopping parameters $\mathcal{T}_{pp}$, $\mathcal{T}_{pd}$ and $\mathcal{T}_{dd}$ lead to a renormalization of each d operator by the factor $\sqrt{Z_B} = \langle 0| \exp(\frac{\lambda}{\omega_0}(b_i - b_i^\dagger))|0\rangle$ so that the hopping part of the one-particle Hamiltonian is renormalized as

$$(p^\dagger d^\dagger) \begin{pmatrix} \mathcal{T}_{pp} & \sqrt{Z_B}\mathcal{T}_{pd} \\ \sqrt{Z_B}\mathcal{T}_{pd}^\dagger & Z_B\mathcal{T}_{dd} \end{pmatrix} \begin{pmatrix} p \\ d \end{pmatrix}, \tag{7}$$

where the site dependence of each orbital species is not explicitly denoted. Equation (7) shows that the bandwidth reduction implied by our effective model happens in a non trivial way in the case of the multi-band models usually dealt with in first-principles calculations.

The arguments we have given are readily generalized to the case of an arbitrary dynamical interaction. The representation of Eq. (1) corresponds to a continuum of boson excitations, $b_i(\nu)$, one for each frequency ν in the screening process, with coupling $\lambda(\nu)$. We then apply a generalized LF transformation obtaining

$$U_0 = V + 2/\pi \int_0^\infty \mathrm{d}\nu \ \mathrm{Im}U_{\mathrm{ret}}(\nu)/\nu, \tag{8}$$

$$Z_B = \exp\left(1/\pi \int_0^\infty \mathrm{d}\nu \ \mathrm{Im}U_{\mathrm{ret}}(\nu)/\nu^2\right). \tag{9}$$

Matching this to the single mode formula implies a characteristic frequency

$$\omega_0 = \frac{\int_0^\infty \mathrm{d}\nu \ \nu \mathrm{Im}U_{\mathrm{ret}}(\nu)/\nu^2}{\int_0^\infty \mathrm{d}\nu \ \mathrm{Im}U_{\mathrm{ret}}(\nu)/\nu^2}. \tag{10}$$

Our theory has important implications for electronic structure calculations for correlated materials. Table (III) presents our results for ω_0, Z_B and U values for a range of compounds calculated using the cRPA method [7], in the implementation of Ref. 17. Typical Z_B values for oxides or pnictides lie in the range of $\sim 0.6 - 0.7$ indicating substantial renormalization of the low energy bandwidths relative to DFT calculations[33], even though the screening frequencies ω_0 are typically high. Standard DFT+DMFT calculations are available for most of the compounds. As shown in Table III, in these calculations, obtaining agreement with experimental results for mass enhancements and metal-insulator phase diagrams has required the use of U values substantially ($\sim 40\%$) larger than the low-frequency Hubbard interactions calculated from cRPA. For example, for $SrVO_3$, LDA+DMFT calculations with U ranging from 4 to 5 eV were found to yield good agreement with experiments [19–21] (instead of the cRPA value of 3.5 eV). Similarly, in VO_2, $U = 4.0$ eV was used [25, 26] instead of $U = 2.7$ eV. We believe that the difference arises because the previous literature did not incorporate the bandwidth reduction effect, and artificially compensated this by increasing U. The one apparent exception is $SrMnO_3$, where the U value quoted in Ref. 27 was chosen to be consistent with the magnetic moment but gaps or other dynamical properties were not studied. A more recent work of a t_{2g}-only model required a rather larger value of 3.5 eV, but overlap with e_g bands precludes a cRPA estimate of Z_B in this case.

Figure 2 shows another illustration of the bandwidth renormalization phenomenon, comparing the spectral function of optimally doped $BaFe_2As_2$ obtained with the "static U" approximation (panel (a)) to the full treatment of the dynamic U, as explained in Ref. 34 (panel (b)), and the effective model (panel (c)). Comparison of panels (a) and (b) shows that screening has a substantial effect on the band structure, shifting the energy positions of bands and band crossings to a significant extent. (The model with screening also has an increased broadening resulting from a change in proximity to a spin freezing line whose position depends very sensitively on parameters [34]; this effect is not of primary interest here). Comparison of panels (b) and (c) shows that the effective model captures the changes in band energies very well, and also reproduces the change in lifetime.

To summarize, in this Letter we showed that the low energy effective Hamiltonian relevant to correlated electron materials involves two renormalizations: a reduction, to a value smaller than the isolated atom value, of the on-site Coulomb interaction and a reduction, to a value smaller than the band theory value, of the bandwidth. The reduction of the onsite Coulomb interaction is a straightforward consequence of screening by high energy degrees of freedom and has been discussed in many works. The reduction of the bandwidth is a more subtle effect, which has important consequences for the low energy physics, including a reduction in the amplitude, and a narrowing of the width of the low-energy part of the electron spectral function, as well as a shift in the location of the metal-insulator transition. We have provided a precise prescription for obtaining the bandwidth reduction and have tested our low-energy effective description against numerically exact dynamical mean field solutions of Hubbard models with full dynamic U in a range of parameters relevant for correlated materials. Important open questions are the issues of full charge-self consistency and the related double counting correction, both of which require knowledge of physics at energy scales above the range of validity of the low-energy effective model. This is the subject of current research.

We acknowledge useful discussions with M. Imada, H. Jiang, I. Krivenko, and G. Sawatzky. This work was supported by the French ANR under project SURMOTT and PNICTIDES, IDRIS/GENCI under Grants 2012096493 and 201201393, SNF Grant PP0022-118866, FOR 1346 and the US DOE under grant BES ER-046169.

[1] W. Kohn, Rev. Mod. Phys. **71**, 1253 (1999).
[2] S. Biermann *"LDA+DMFT" - a Tool for Investigating the Electronic Structure of Materials with Strong Electronic Coulomb Correlations*, in Encyclopedia of Materials: Science and Technology. Ed. by J. Buschow, Elsevier 2005.
[3] K Held *et al*. J. Phys.: Cond. Matter **20**, 064202 (2008).
[4] G. Kotliar, S. Y. Savrasov, K. Haule, V. S. Oudovenko, O. Parcollet, and C. A. Marianetti, Rev. Mod. Phys. **78**, 865 (2006).
[5] O. Gunnarsson, O. K. Andersen, O. Jepsen, and J. Zaanen, Phys. Rev. B **39**, 1708 (1989).
[6] M. Cococcioni and S. de Gironcoli, Phys. Rev. B **71**, 035105 (2005).
[7] F. Aryasetiawan, M. Imada, A. Georges, G. Kotliar, S. Biermann, and A. I. Lichtenstein, Phys. Rev. B**70**, 195104 (2004).
[8] Y. Imai, I. Solovyev, and M. Imada, Phys. Rev. Lett. **95**, 176405 (2005).
[9] M. Berciu, I. Elfimov, and G. A. Sawatzky, Phys. Rev. B **79**, 214507 (2009).
[10] J. E. Hirsch, Phys. Rev. Lett. **87**, 206402 (2001).
[11] Y. Takada and A. Chatterjee, Phys. Rev. B **67**, 081102 (R) (2003).
[12] A. Macridin, G. A. Sawatzky, M. Jarrell Phys. Rev. B **69**, 245111 (2003).
[13] I. G. Lang and Y. A. Firsov, Sov. Phys. JETP **16**, 1301 (1962).
[14] P. Werner and A. J. Millis, Phys. Rev. Lett. **99**, 146404 (2007).
[15] P. Werner and A. J. Millis, Phys. Rev. Lett. **104**, 146401 (2010).
[16] M. Casula, A. Rubtsov, and S. Biermann, Phys. Rev. B **85**, 035115 (2012).
[17] L. Vaugier, PhD thesis, Ecole Polytechnique (2011), L. Vaugier, H. Jiang, S. Biermann, arXiv:1206.3533 (2012).
[18] M. Aichhorn, et al., Phys. Rev. B **80**, 085101 (2009).
[19] A. Liebsch, Phys. Rev. Lett. **90**, 096401 (2003)
[20] E. Pavarini, S. Biermann, A. Poteryaev, A. I. Lichtenstein, A. Georges, and O. K. Andersen, Phys. Rev. Lett. **92**, 176403 (2004).
[21] A. Sekiyama, et al., Phys. Rev. Lett. **93**, 156402 (2004).
[22] F. Lechermann, A. Georges, A. Poteryaev, S. Biermann, M. Posternak, A. Yamasaki, and O. K. Andersen, Phys. Rev. B **74**, 125120 (2006).
[23] R. Arita et al., J. Phys. : Cond. Matter **19**, 365204 (2007).
[24] M. De Raychaudhury, E. Pavarini, and O. K. Andersen, Phys. Rev. Lett. **99**, 126402 (2007).
[25] S. Biermann et al., Phys. Rev. Lett. **94**, 026404 (2005).
[26] J. M. Tomczak and S. Biermann, Europhys. Lett. **86** 3 (2009) 37004, Phys. Rev. B 80, 085117 (2009).
[27] J. Hee Lee and K. M. Rabe, Phys. Rev. Lett. **104**, 207204 (2010)
[28] Z. P. Yin, K. Haule and G. Kotliar, Nature Materials **10**, 932 (2011), A. Kutepov et al., Phys. Rev. B **82**, 045105 (2010).
[29] K. Haule, J. H. Shim and G. Kotliar, Phys. Rev. Lett. **100**, 226402 (2008).
[30] V. I. Anisimov et al., J. Phys. : Cond. Matter **21**, 075602 (2009).
[31] L. Craco et al., Phys. Rev. B **78**, 134511 (2008).
[32] D. Wu et al., Phys. Rev. B **73**, 235206 (2006).
[33] The band dispersion may experience further modification due to the k-dependence of the self-energy which has not been taken into account.
[34] P. Werner, *et al.*, Nature Physics **8**, 331 (2012).

Figures

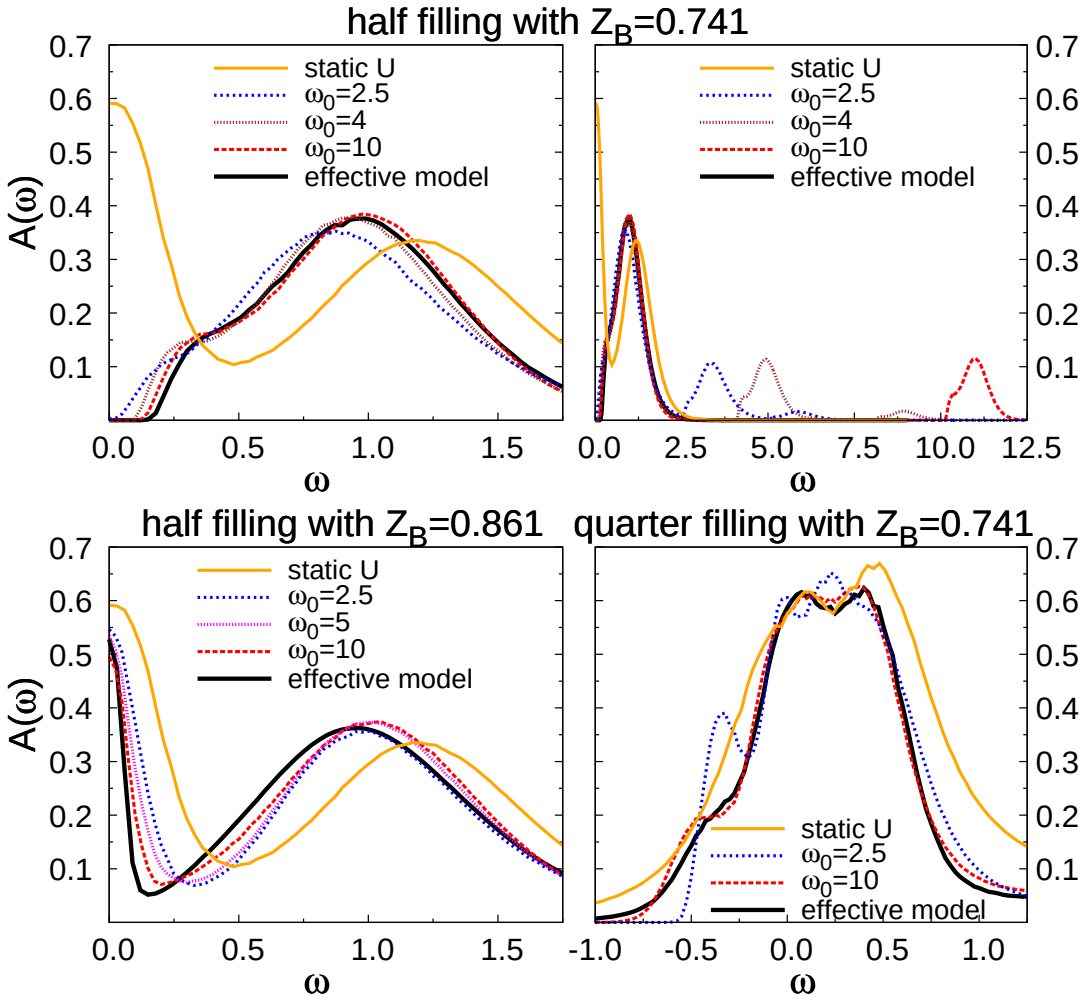

FIG. 1: Spectral functions computed from Eq. (2) at various screening frequencies ω_0 with $\beta = 40$, screened interaction $U_0 = 2$ and coupling constants chosen to produce the renormalization factor Z_B as indicated. Also shown are the spectral functions computed from the effective model (Eq. (6)) and for the static U approximation.

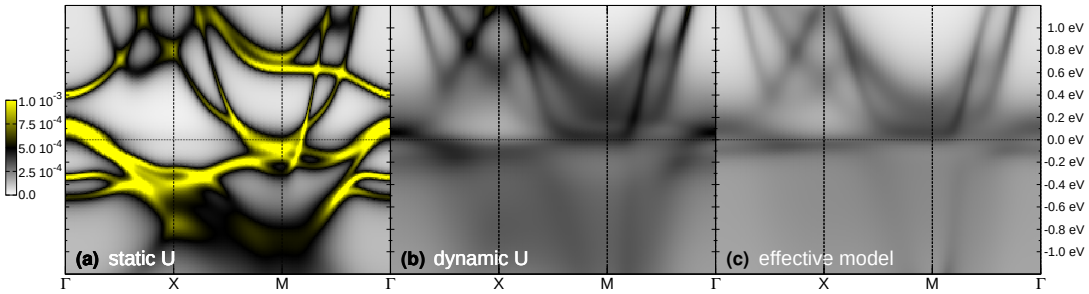

FIG. 2: k-resolved spectral function for $K_xBa_{(1-x)}Fe_2As_2$ at optimal doping $x = 0.4$ and $\beta = 20\text{eV}^{-1}$, reported for a static U standard DMFT calculation (panel (a)), the DMFT calculation with dynamic $U(\omega)$ (panel (b)), and the DMFT calculation for our effective low-energy model. In all calculations, the static limit of $U(= F_0)$ is $U(0) = 2.84$ eV, and $J = 0.68$ eV. In the effective model, the double counting correction is set to match the d-electron number of the dynamical calculation.

Tables

TABLE I: Critical interaction strength $U_{\text{crit}}^{\text{exact}}$ (presented in terms of zero frequency screened value) needed to drive the metal insulator transition obtained from the single-site DMFT approximation to Eq. (2) at inverse temperature $\beta = 100$ and compared to the estimate $U_{\text{crit}}^{\text{eff}}$ for different values of the screening frequency ω_0 and strength λ. Also shown is the Lang-Firsov renormalization factor $Z_B = \exp[-\lambda^2/\omega_0^2]$.

ω_0	λ	Z_B	$U_{\text{crit}}^{\text{exact}}$ [15]	$U_{\text{crit}}^{\text{eff}}$
1.5	0.820	0.74	2.103	1.891
1.5	2.010	0.17	0.613	0.423
2.5	1.330	0.75	2.085	1.921
2.5	2.770	0.29	0.861	0.747
10.0	3.725	0.87	2.225	2.220
10.0	6.465	0.66	1.640	1.679

TABLE II: Quasiparticle residue $a = 1/(1 - \partial \text{Im}[\Sigma(i\omega)]/\partial\omega|_{\omega=0})$ computed from the effective Hamiltonian Eq. (4) with screened $U_0 = 2$, and different ω_0, Z_B and particle density as shown. The values in parenthesis give the relative discrepancy $|a(\omega_0)/a(\omega_0 \to \infty) - 1|$. Note that the static model without bandwidth reduction (last row) is substantially incorrect.

	half-filling	quarter-filling	
	Z_B=0.861	Z_B=0.861	Z_B=0.741
$\omega_0 = 2.5$	0.137 (0.37)	0.635 (0.04)	0.560 (0.10)
$\omega_0 = 3$	0.125 (0.32)	0.631 (0.03)	0.551 (0.08)
$\omega_0 = 10$	0.091 (0.06)	0.604 (0.01)	0.509 (0.01)
$\omega_0 = \infty$	0.085	0.609	0.504
static U	0.253	0.713	0.713

TABLE III: Boson renormalisation factor Z_B, characteristic frequency ω_0 [eV], bare interaction V [eV], zero-frequency screened interaction U_0 [eV] as calculated within the cRPA, in the implementation of Ref. [17]. For the oxide and sulfide compounds (except $SrMnO_3$), data refer to a model comprising only the t_{2g} states, where U is defined as the average over the diagonal entries of the Hubbard interaction matrix U_{mmmm}. For the pnictide compounds, as well as for $SrMnO_3$ and CuO, a hybrid "d-dp" model in the notation of Ref. [17, 18] was constructed and $U(= F_0)$ is defined as the average over all density-density interaction matrix elements. Experimental lattice structures (rutile in the case of VO_2, hexagonal lattice in the case of TaS_2) were used except in the cases of Sr_2VO_4, $LaVO_3$ and $SrMnO_3$, where an undistorted (double) perovskite structure was adopted. The column headed U_{lit} gives U values obtained via a variety of methods other than cRPA claimed in the literature to give quantitative agreement with experiment when used in DFT+DMFT (oxides, sulfides and pnictides) or DFT+U calculations ($SrMnO_3$ and CuO) within the same correlated subspace, but without the band renormalization physics.

	Z_B	ω_0	V	U_0	U_{lit}	
$SrVO_3$	0.70	18.0	16.5	3.3	4 - 5	[19–22]
Sr_2VO_4	0.70	18.1	15.7	3.1	4.2	[23]
$LaVO_3$	0.57	10.3	13.3	1.9	5	[24]
VO_2	0.67	15.6	15.2	2.7	4	[25, 26]
TaS_2	0.79	14.7	8.4	1.5		
$SrMnO_3$	0.50	13.3	21.6	3.1	2.7	[27]
$BaFe_2As_2$	0.59	15.7	19.7	2.8	5	[28]
LaOFeAs	0.61	16.5	19.1	2.7	3.5 - 5	[28–30]
FeSe	0.63	17.4	20.7	4.2	4 - 5	[28, 31]
CuO	0.63	21.1	26.1	6.8	7.5	[32]